doi:10.1038/nature09958

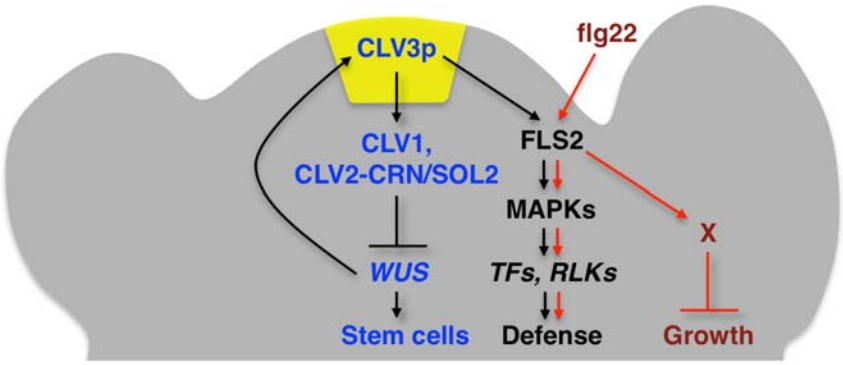

Supplementary Figure 1 | Model of CLV3p and flg22 signalling in the *Arabidopsis* SAM. CLV3p, which is expressed and secreted from stem cells (yellow region), suppresses the *WUS* expression through the CLV1 and CLV2-CRN/SOL2 receptors. CLV3p and flg22 activate the FLS2 receptor and share MAPK and immune marker gene activation in the SAM. TF: transcription factor; RLK: receptor-like kinase. The growth suppression of seedling is only triggered by flg22 through unknown downstream components (X). Black lines represent CLV3p signalling pathways and red lines indicate flg22-activated pathways.

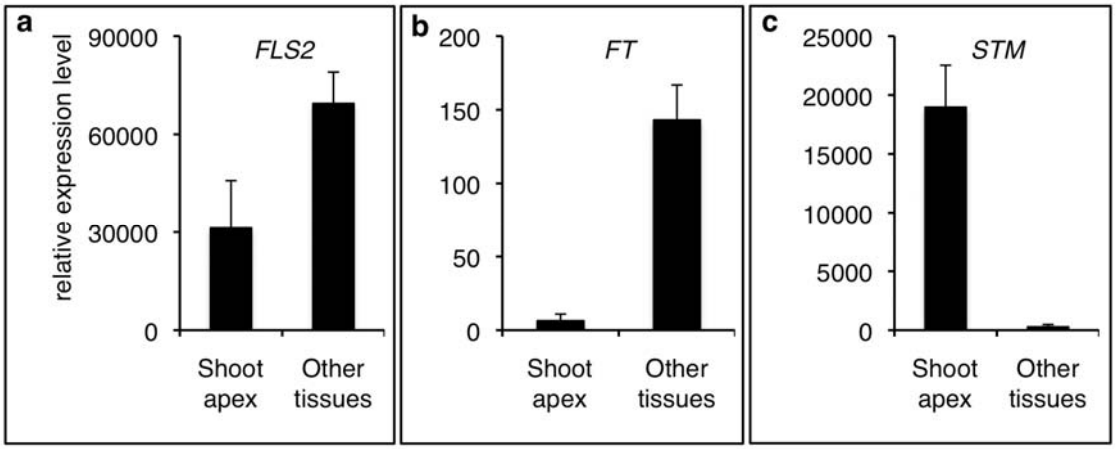

Supplementary Figure 2 | ***FLS2* expression in the SAM.** Relative expression levels of *FLS2* (**a**), *FT* (**b**) and *STM* (**c**) were analyzed by quantitative RT-PCR in the shoot apex and the rest of tissues (Other tissues) of 7-day-old L*er* seedlings. *FLS2* is highly expressed in both shoot apex and other tissues. *FT* (*FLOWERING LOCUS T*) is mainly expressed in leaves in response to day length. Because *FT* mRNA accumulation is hardly detectable in the SAM of *Arabidopsis* and rice[1,2], the shoot apex tissues used in this study are not contaminated with leaf tissues. The SAM marker gene *STM* (*SHOOT MERISTEMLESS*) is only expressed in the shoot apex but not other tissues. The relative expression level of each gene was normalized by *ACT2*. Error bars, s.d. (*n*=4).

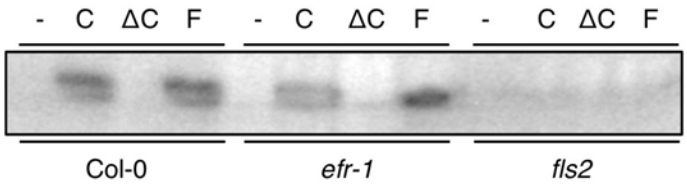

Supplementary Figure 3 | CLV3p activation of MAPK requires the FLS2 but not EFR receptor. In-gel MAPK assay based on MBP phosphorylation was examined in Col-0, *efr-1* and *fls2* protoplasts treated with 1 μM CLV3p (C), 1 μM ΔCLV3 (ΔC) or 100 nM flg22 (F) for 10 min. Control (−) has no peptide.

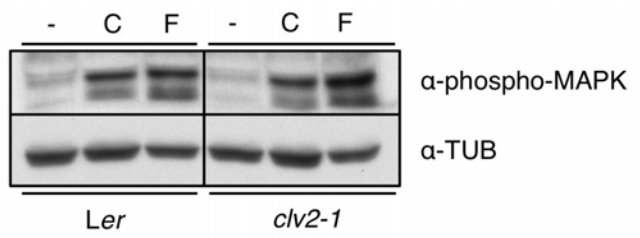

Supplementary Figure 4 | CLV3p-induced MAPK activation is not affected in the *clv2-1* mutant. Activated MAPKs were detected by an anti-phospho-MAPK antibody in immunoblot analysis. Protoplasts were isolated from L*er* and *clv2-1* leaves and treated with 1 μM CLV3p (C) or 100 nM flg22 (F) for 10 min. Control (−) has no peptide. Quantity of total protein was compared by an anti-TUB antibody in immunoblot analysis.

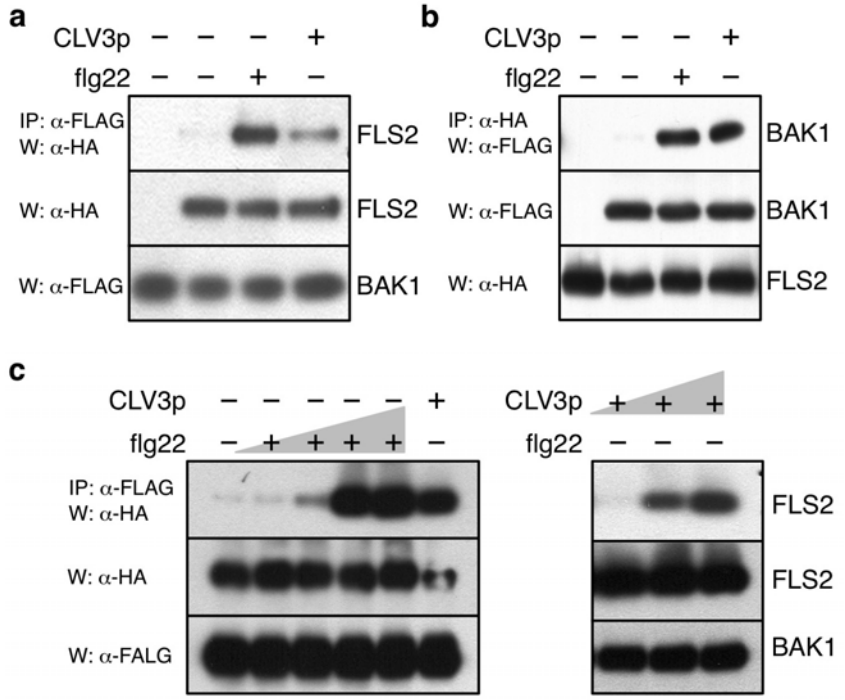

Supplementary Figure 5 | **Flg22 is more potent than CLV3p. a**, FLS2-BAK1 interaction induced by CLV3p. Protoplasts coexpressing FLS2-HA and BAK1-FLAG were treated with 1 μM CLV3p or 100 nM flg22 for 10 min (**a**, **b**). The co-IP (top) was first performed with an anti-FLAG antibody (α –FLAG) and then examined using an anti-HA antibody (α-HA) by immunoblot analysis. Input FLS2-HA (middle) and BAK1-FLAG (bottom) proteins were detected by immunoblot analysis. **b**, Reciprocal co-IP assay of FLS2-BAK1 interaction. Co-IP by anti-HA antibody (α-HA) was detected by anti-FLAG antibody (α-FLAG). Top, co-IP. Middle, Immunoblot analysis of BAK1-FLAG. Bottom, Immunoblot analysis of FLS2-HA. **c**, FLS2-BAK1 interaction in the condition of various flg22 and CLV3p concentrations. The activity of flg22 (0.01, 0.1, 1, 10 nM) and 1 μM CLV3p (left) or different concentrations of CLV3p (0.1, 1 and 10 μM) (right) was examined using the co-IP assay for ligand-triggered FLS2-BAK1 interaction. Top, co-IP. Middle, Immunoblot analysis of FLS2-HA. Bottom, Immunoblot analysis of BAK1-FLAG.

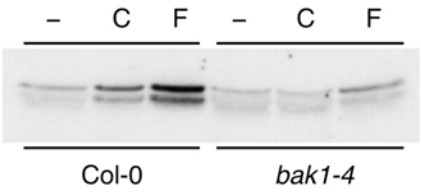

Supplementary Figure 6 | CLV3p-mediated MAPK activation is impaired in *bak1-4*. In-gel MAPK assay based on MBP phosphorylation was examined in Col-0 and *bak1-4* protoplasts treated with 1 μM CLV3p (C) or 100 nM flg22 (F) for 10 min. Control (−) has no peptide.

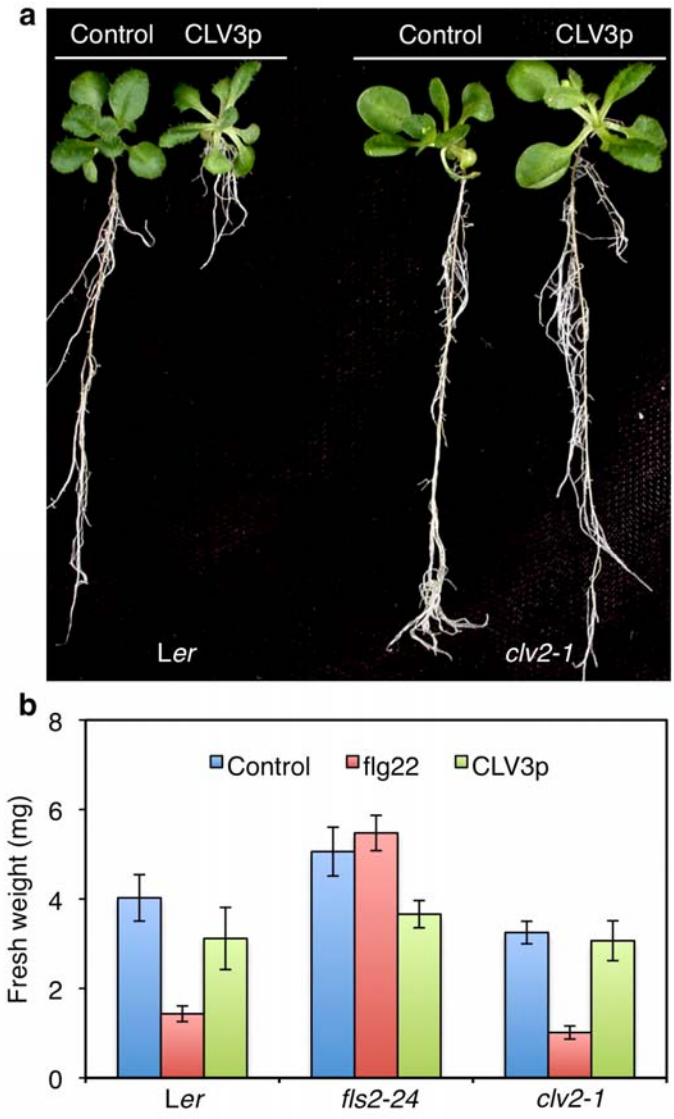

Supplementary Figure 7 | **Differential regulation of seedling growth by flg22 and CLV3p. a**, CLV3p inhibition. L*er* and *clv2-1* seedlings were grown vertically on medium plates (0.5 x MS, 1 % sucrose and 0.6 % phytoagar) for 17 days with 1 μM CLV3p. Control has no peptide. **b**, Differential effects of flg22 and CLV3p on seedling growth. L*er*, *fls2-24* or *clv2-1* seedlings were grown in liquid medium for 6 days with 10 nM flg22 or 1 μM CLV3p. Fresh weight was measured from eight seedlings. Error bars, s.d. (*n*=8). Experiments were repeated twice with similar results.

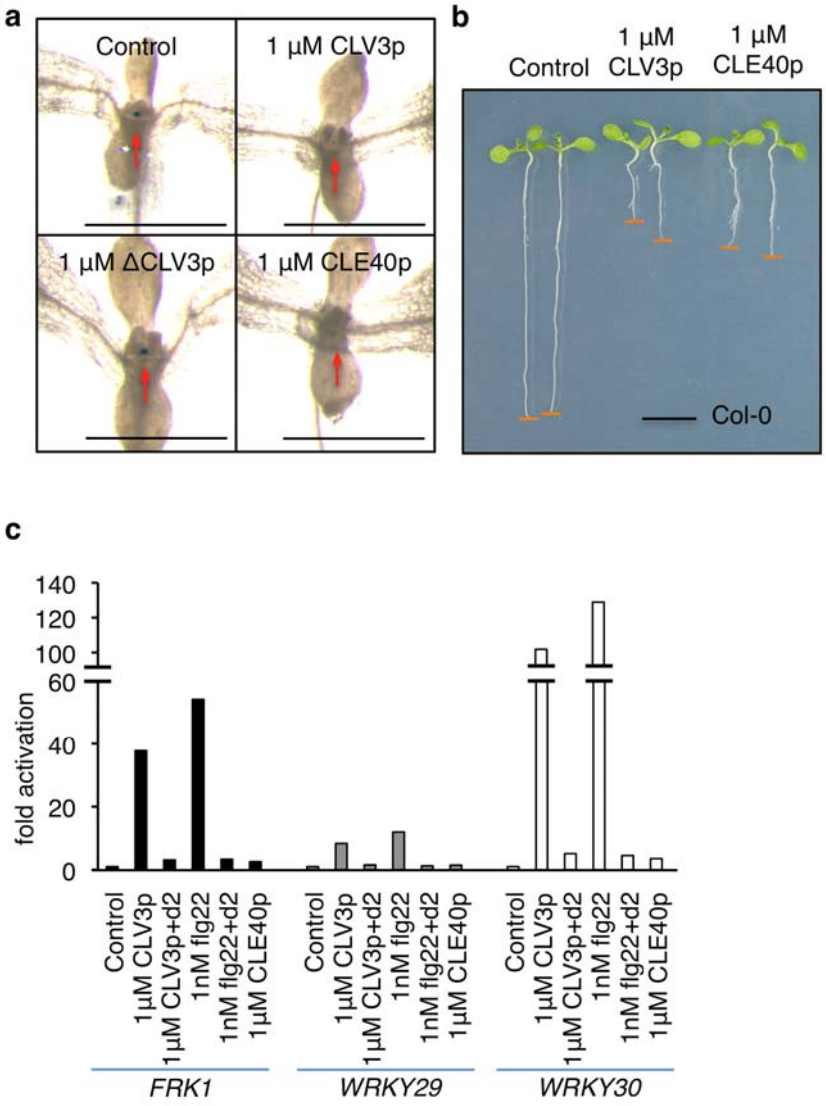

Supplementary Figure 8 | **CLE40p does not stimulate innate immune signalling. a**, CLE40p represses *WUS* in the SAM. Seedlings harboring *pWUS::GUS* were grown in liquid medium for 8 days with 1 µM CLV3p, 1 µM ΔCLV3p or 1 µM CLE40p. Control has no peptide. Red arrows indicate GUS signals that represent *WUS* expression. **b**, CLE40p inhibits root growth. Seedlings were grown with 1 µM CLV3p or 1 µM CLE40p for 8 days. Scale bars, 1 cm (**a, b**). **c**, Quantitative RT-PCR analysis of early flg22 marker gene activation in protoplasts. Samples were collected after treatment with 1 µM CLV3p, 1 µM CLE40p or 1 nM flg22 for 1 h. The 50 µM of antagonistic peptide flg22-Δ2 (d2) was added in CLV3p and flg22 competition experiments.

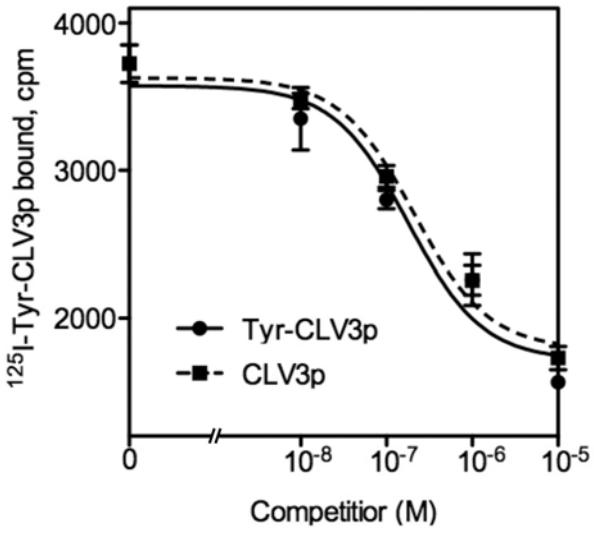

Supplementary Figure 9 | The binding of ^{125}I-Tyr-CLV3p to FLS2 receptor is similarly diminished by CLV3p and Tyr-CLV3p. FLS2-HA was expressed in *fls2* protoplasts (2.5 x 10^5 cells) for 6 h. Total extracts were prepared from protoplasts to perform ^{125}I-Tyr-CLV3p (1 nM) binding assay without (0) or with 0.1, 1 or 10 μM cold Tyr-CLV3p or CLV3p for 30 min on ice. ^{125}I-Tyr-CLV3p bound extracts were collected by vacuum filtration through glass fiber filter and washed with cold binding buffer. The radioactivity was determined by a gamma counter. Error bars, s.d. (*n*=3). The cpms retained on the filter in assays with 10 μM of unlabeled Tyr-CLV3p or CLV3p peptides represented the non-specific ^{125}I-Tyr-CLV3p binding background as also shown in Fig. 2d and 2f. The competition data with CLV3p was obtained in the same set of experiments with the other unlabeled peptides shown in Fig. 2f. This figure provides a clear visualization of the competition data with CLV3p and Tyr-CLV3p by avoiding extensive overlaps with the flg22 competition data shown in Fig. 2f. The data for Tyr-CLV3p competition are identical to the data shown in Fig 2f to serve as a reference for direct comparison between Fig. 2f and Supplementary Fig. 8.

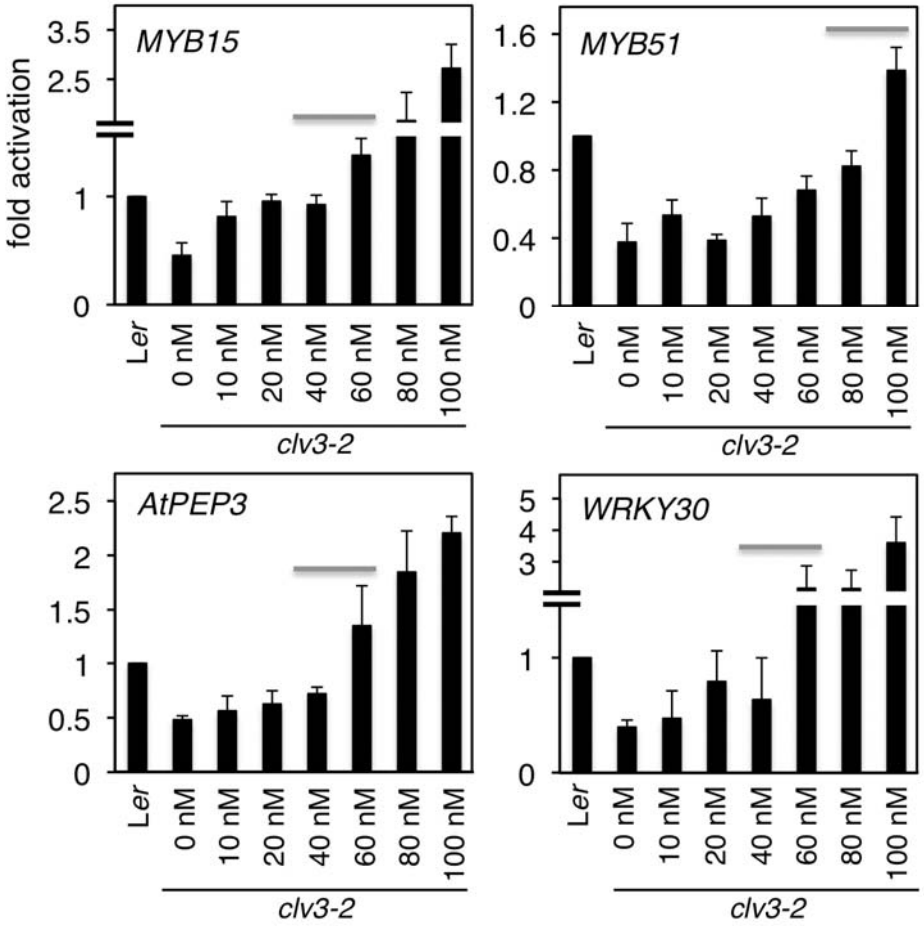

Supplementary Figure 10 | **Endogenous levels of immune marker genes in the SAM of *clv3-2* were complemented by exogenous CLV3p.** L*er* and *clv3-2* seedlings were grown in liquid medium (0.5 x MS, 0.5 % sucrose) for 7 days. *clv3-2* seedlings were treated with 0, 10, 20, 40, 60, 80 or 100 nM CLV3p for 1 h and immediately frozen by liquid nitrogen. SAM tissues were harvested and endogenous levels of immune marker genes were analyzed by qRT-PCR. Error bars, s.d. (n=3). The expression of each gene was normalized based on *ACT2*. The grey bar marks the exogenous CLV3p concentration required for complementation of immune marker gene expression in the SAM of *clv3-2*.

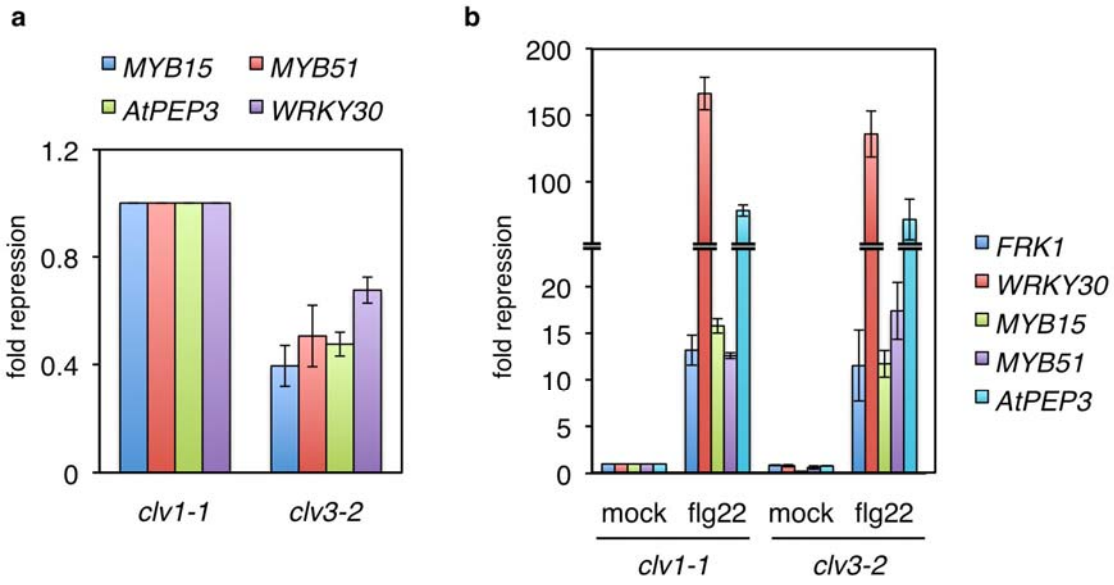

Supplementary Figure 11 | The expression of immune marker genes in the SAM of *clv3-2* mutant. Analysis of steady state level (**a**) and flg22 induction (**b**) of the endogenous immune marker gene expression in the SAM tissues of *clv1-1* and *clv3-2* seedlings by qRT-PCR. The *clv1-1* mutant was used as a control with similarly enlarged SAM size. The SAM tissue was treated with 1 nM flg22 for 1 h (**b**). Error bars, s.d. (n=3). The expression of each gene was normalized based on *ACT2*.

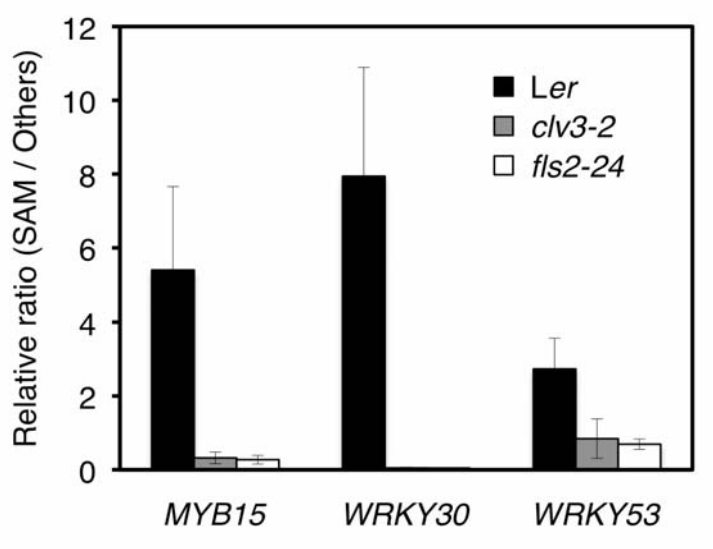

Supplementary Figure 12 | **Endogenous immune marker genes are constitutively expressed at higher levels in the SAM.** Endogenous expression levels of immune marker genes in the SAM tissues of L*er*, *clv3-2* and *fls2-24* seedlings were compared to those in the rest of tissues (Others) from 7-day-old seedlings by qRT-PCR. Error bars, s.d. (*n*=3). The expression of each gene was normalized based on *ACT2*, which is expressed similarly in all tissues of WT (L*er*) and mutants.

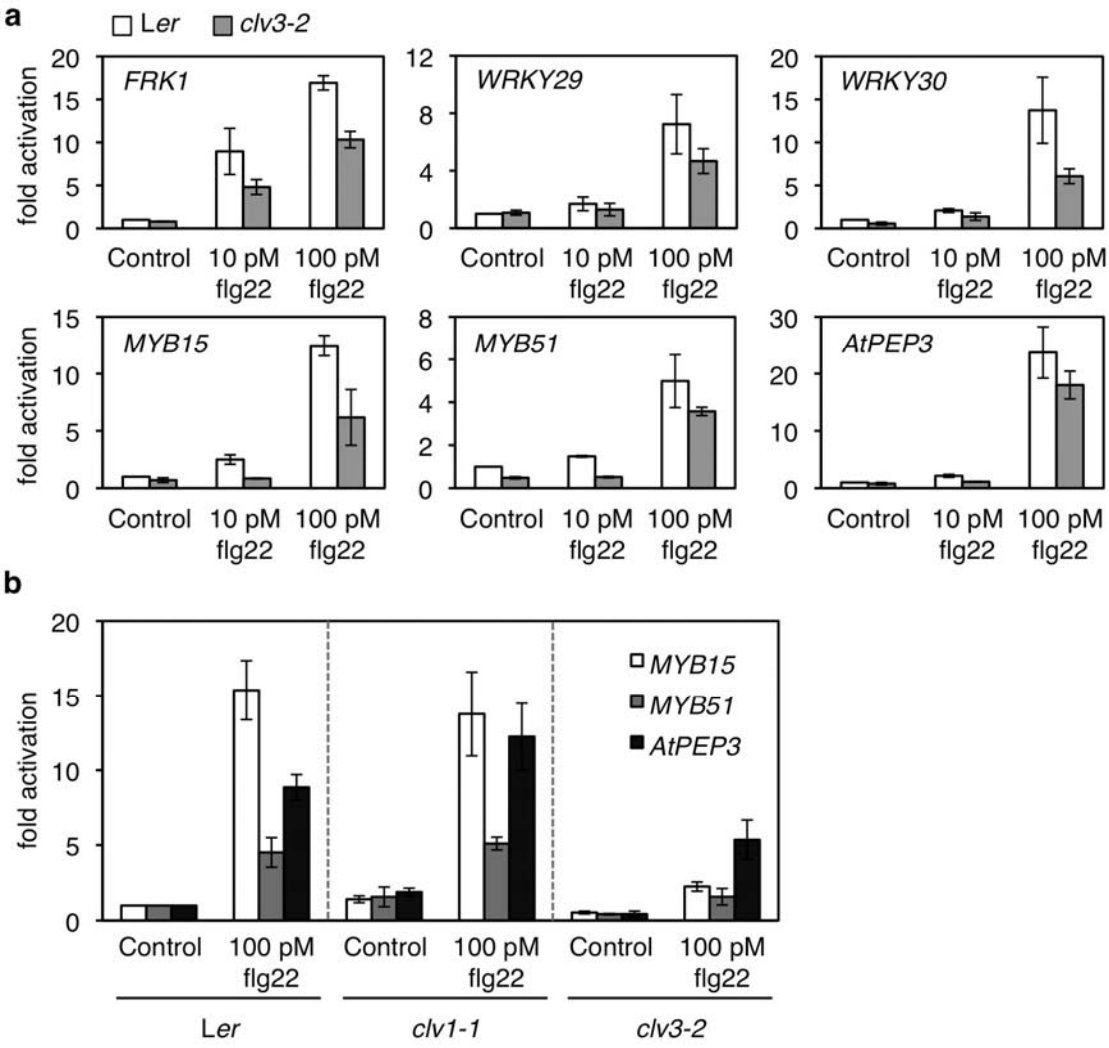

Supplementary Figure 13 | **Flg22 induction of immune marker genes in the SAM of *clv3-2* mutant.** (**a**) The expression of immune marker genes in the SAM was reduced in *clv3-2* (gray bar) compared to that in L*er* (white bar). (**b**) The expression of immune marker genes in the SAM was not reduced in *clv1-1*. Seedlings were grown in liquid medium (0.5 x MS, 0.5 % Sucrose) for 7 days and treated without (Control) or with 10 pM or 100 pM flg22 for 1 h. Error bars, s.d. (n=3). The expression of each gene was normalized based on *ACT2*.

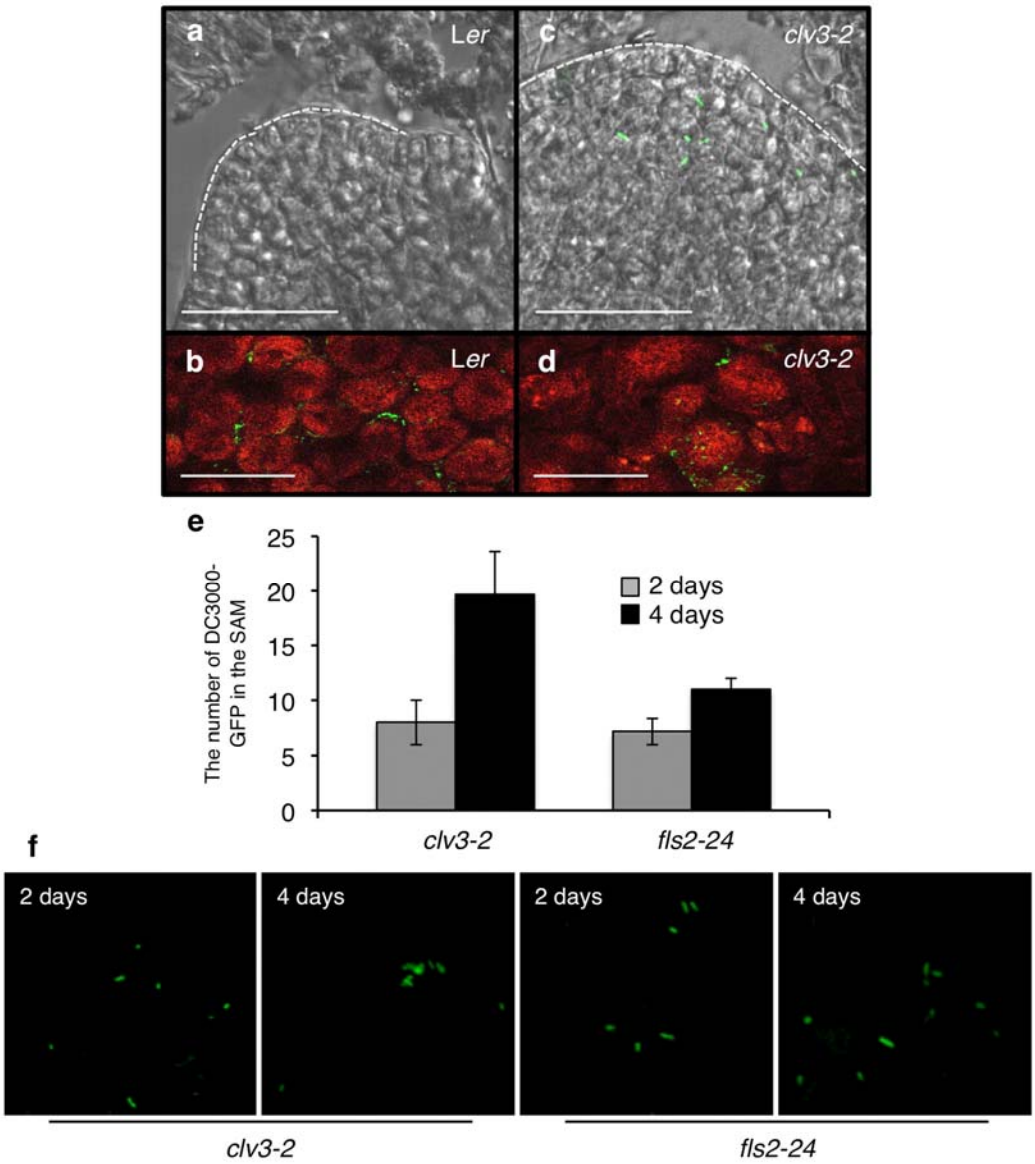

Supplementary Figure 14 | SAM immunity is impaired in the *clv3-2* and *fls2-24* mutant. Visualization of bacterial infection was performed with *Pst* DC3000-GFP in L*er* (**a**, **b**) or *clv3-2* seedlings (**c**, **d**). Co-cultivation was carried out for 2 days before *Pst* DC3000-GFP visualization in the SAM (**a**, **c**) or cotyledons (**b**, **d**) using a confocal microscope. Scale bars, 50 μm (**a**-**d**). The red autofluorescence is from chlorophyll. The experiment was repeated three times with similar results. **e**, The number of bacteria in the infected SAM. Error bars, s.d. (*n*=5). **f**, High magnification of *Pst* DC3000-GFP in the SAM of *clv3-2* and *fls2-24* mutants. Pictures were cropped from Fig. 4c.

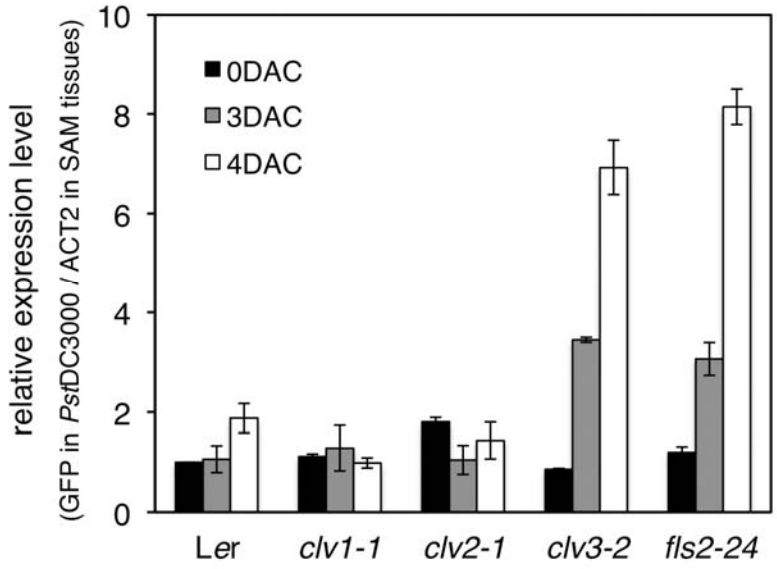

Supplementary Figure 15 | **Bacterial growth in the SAM was analyzed by quantitative PCR.** The infection of *Pst*DC3000-GFP in the SAM region was quantified by qPCR using GFP specific primers and DNA from bacteria and plants. Nine seedlings were grown in liquid medium (0.5 x MS, 0.5 % Sucrose) for 2 days and co-cultivated with 200 µl of *Pst*Dc3000-GFP (OD_{600} = 0.5) for 3 or 4 days. After washing and rinsing seedlings twice, tissues from five SAMs were harvested and ground in 100 µl of water. Control experiments were conducted at 0 DAC (day after co-cultivation) to determine non-specific bacterial attachment 1 h after co-cultivation (black bar). Error bars, s.d. (*n*=3). The GFP level determined by qPCR was correlated with specific bacterial growth in *clv3-2* and *fls2-24* normalized based on the *Arabidopsis ACT2* gene in the SAM tissues. *Pst*DC3000-GFP only proliferated and grew significantly in the SAM of *clv3-2* and *fls2-24* mutants at 3 and 4 DAC (grey and white bar, respectively). No *Pst*DC3000-GFP was observed in the SAM of Ler, *clv1-1* and *clv2-1* as shown in Fig. 4c.

Supplementary Table 1 | Name and sequence of peptides used in this study.

Peptides were synthesized using the MGH Peptide/Protein Core Facility (Charlestown, MA). Three other peptide services were also used. The CLV3p used in this study is identical to the endogenous modified CLV3 peptide identified by in situ MALDI-TOF MS analysis[3]. For direct binding analysis, ^{125}I-Tyr-CLV3p and Tyr-CLV3p were synthesized and labeled in five independent batches by Phoenix Pharmaceuticals, Inc.

Name	Sequence
CLV3 peptide (CLV3p)	RTVP^{h}SGP^{h}DPLHH[3]
Inactive CLV3 peptide (ΔCLV3p)	RTVP^{h}SGP^{h}DPLH[3]
Tyr-CLV3p	YRTVP^{h}SGP^{h}DPLHH
flg22 peptide	QRLSTGSRINSAKDDAAGLQIA[4]
flg22-Δ2 peptide	QRLSTGSRINSAKDDAAGLQ[4]
CLE40 peptide (CLE40p)	RQVP^{h}TGSDPLHH[5]

*P^{h} is Hydroxyproline.

Supplementary Table 2 | Primers used for qRT-PCR.

Name	Forward primer	Reverse primer
FRK1 (At2g19190)	ATCTTCGCTTGGAGCTTCTC	TGCAGCGCAAGGACTAGAG
WRKY29 (At4g23550)	CTCCATACCCAAGGAGTTATTACAG	CGGGTTGGTAGTTCATGATTG
WRKY30 (At5g24110)	GCAGCTTGAGAGCAAGAATG	AGCCAAATTTCCAAGAGGAT
WRKY53 (At4g23810)	AAACTGTTGGGCAACGAAAC	GGCTGGTTTGACTCTGGTGT
MYB15 (At3g23250)	TCACCAAAGAAGAGGAAGATGC	TTGTTGCTGGTCTTAGGTTTAGC
MYB51 (At1g18570)	TGGGCCAATTATCTTAGACCTG	TGATCTCGTTATCGGTTCTTCC
AtPEP3 (At5g64905)	TCCGGTCTCGAAAGTTCATC	CTCATCTTCCTCGCTGTGTG
WUS (At2g17950)	TGCAAGCTCAGGTACTGAATG	ATGATCCATGTTTGCCCATC
FLS2 (At5g46330)	AGCGCACGACAATCTTCTTACCG	ATCTCGCCAGTCATTTGGTTGTGAG
FT (At1g65480)	AGGCCTTCTCAGGTTCAAAACAAGC	TGCCAAAGGTTGTTCCAGTTGTAGC
STM (At1g62360)	TCATGGCTCATCCTCACTACC	CCTGTTGGTCCCATAGATGC
ACT2 (At3g18780)	TCCCTCAGCACATTCCAGCAGAT	AACGATTCCTGGACCTGCCTCATC
DC3000-GFP[6]	TGGAAGCGTTCAACTAGCAG	AAAGGGCAGATTGTGTGGAC

Supplementary References

1. Corbesier, L., et al. FT protein movement contributes to long-distance signaling in floral induction of *Arabidopsis*. *Science* **316**, 1030-1033 (2007).

2. Tamaki, S. et al. Hd3a protein is a mobile flowering signal in rice. *Science* **316**, 1033-1036 (2007).

3. Kondo, T. et al. A plant peptide encoded by CLV3 identified by in situ MALDI-TPF MS analysis. *Science* **313**, 845-848 (2006).

4. Chinchila, D., Bauer, Z., Regenass, M., Boller, T. & Felix, G. The *Arabidopsis* receptor kinase FLS2 binds flg22 ad determines the specificity of flagellin perception. *Plant Cell* **18**, 465-476 (2006).

5. Jun, J. H., Fiume, E. & Fletcher, J. C. The CLE family of plant polypeptide signaling molecules. *Cell. Mol. Life Sci.* **65**, 743-755 (2008).

6. Prasher, D. C., Eckenrode, V. K., Ward, W. W., Prendergast, F. G. & Cormier, M. J. Primary structure of the *Aequorea Victoria* green-fluorescent protein. *Gene* **111**, 229-233 (1992).